Kinetic Analysis of cAMP-activated Na^+ Current in the Molluscan Neuron

A Diffusion–Reaction Model

RONG-CHI HUANG and RHANOR GILLETTE

From the Department of Physiology and Biophysics, University of Illinois, Urbana, Illinois 61801

ABSTRACT cAMP-activated Na^+ current ($I_{Na,cAMP}$) was studied in voltage-clamped neurons of the seaslug *Pleurobranchaea californica*. The current response to injected cAMP varied in both time course and amplitude as the tip of an intracellular injection electrode was moved from the periphery to the center of the neuron soma. The latency from injection to peak response was dependent on the amount of cAMP injected unless the electrode was centered within the cell. Decay of the $I_{Na,cAMP}$ response was slowed by phosphodiesterase inhibition. These observations suggest that the kinetics of the $I_{Na,cAMP}$ response are governed by cAMP diffusion and degradation. Phosphodiesterase inhibition induced a persistent inward current. At lower concentrations of inhibitor, $I_{Na,cAMP}$ response amplitude increased as expected for decreased hydrolysis rate of injected cAMP. Higher inhibitor concentrations decreased $I_{Na,cAMP}$ response amplitude, suggesting that inhibitor-induced increase in native cAMP increased basal $I_{Na,cAMP}$ and thus caused partial saturation of the current. The Hill coefficient estimated from the plot of injected cAMP to $I_{Na,cAMP}$ response amplitude was close to 1.0. An equation modeling $I_{Na,cAMP}$ incorporated terms for diffusion and degradation. In it, the first-order rate constant of phosphodiesterase activity was taken as the rate constant of the exponential decay of the $I_{Na,cAMP}$ response. The stoichiometry of $I_{Na,cAMP}$ activation was inferred from the Hill coefficient as 1 cAMP/channel. The equation closely fitted the $I_{Na,cAMP}$ response and simulated changes in the waveform of the response induced by phosphodiesterase inhibition. With modifications to accommodate asymmetric $I_{Na,cAMP}$ activation, the equation also simulated effects of eccentric electrode position. The simple reaction–diffusion model of the kinetics of $I_{Na,cAMP}$ may provide a useful conceptual framework within which to investigate the modulation of $I_{Na,cAMP}$ by neuromodulators, intracellular regulatory factors, and pharmacological agents.

INTRODUCTION

cAMP-activated Na^+ current ($I_{Na,cAMP}$) is prominent in many molluscan neurons (Liberman et al., 1975; Deterre et al., 1981; Aldenhoff et al., 1983; Green and Gillette,

Address reprint requests to Dr. Rhanor Gillette, Department of Physiology and Biophysics, 524 Burrill Hall, 407 S. Goodwin Ave., University of Illinois, Urbana, IL 61801.

J. GEN. PHYSIOL. © The Rockefeller University Press · 0022-1295/91/10/0835/14 $2.00 835
Volume 98 October 1991 835–848

1983; Kononenko et al., 1983; Connor and Hockberger, 1984; Hara et al., 1985; Swandulla, 1987; McCrohan and Gillette, 1988*a*). The current contributes to neuromodulatory responses (Huang and Gillette, 1987) and paroxysmal activity (McCrohan and Gillette, 1988*b*). In some neurons, $I_{Na,cAMP}$ is coregulated by Ca^{2+} and intracellular pH (Gillette and Green, 1987; Green and Gillette, 1988; Gillette and Huang, 1988).

The kinetics and mechanisms of $I_{Na,cAMP}$ have been partly characterized. The $I_{Na,cAMP}$ response to cAMP injection is characterized by a slow time course. Peak response may be attained with a delay of several seconds after cAMP injection and has a similarly slow decay rate. The current is resistant to inhibitors of cAMP-dependent protein kinase and can be activated in the inside-out patch by cAMP in the absence of ATP (Huang and Gillette, 1989). Evidence from the use of phosphodiesterase (PDE) inhibitors and nonhydrolyzable cAMP analogues has suggested that decay of $I_{Na,cAMP}$ is due to in situ PDE activity, rather than to a mechanism of channel inactivation (Aldenhoff et al., 1983; Connor and Hockberger, 1984).

Here we describe the theory and experiment characterizing the contributions of diffusion and cAMP degradation to the $I_{Na,cAMP}$ response to pulse injection of cAMP. A simple set of equations is presented that was elaborated from the experimental data, diffusion theory, and enzyme kinetics. The equations and experimental results define the relationships among cAMP concentration at the membrane, the magnitude of $I_{Na,cAMP}$, diffusion, hydrolysis, current saturation, and point source of cAMP injection.

MATERIALS AND METHODS

Experimental Technique

Specimens of *Pleurobranchaea californica* were provided by R. Fay of Pacific BioMarine, Venice, CA, and M. Morris of Sea-life Supply, Sand City, CA, and were maintained in artificial sea water at 13–15°C. Pedal ganglia were dissected into saline where a group of 8–10 large and spherical (100–300 μm diam) neuron somata was isolated and stabilized on Sylgard with insect pins. While differing somewhat in axon paths and spontaneous activity in situ, the neurons have in common a $I_{Na,cAMP}$ sensitive to low iontophoretic currents of cAMP. Extracellular saline composition was (in mM): 420 NaCl, 25 $MgSO_4$, 25 $MgCl_2$, 10 KCl, 10 $CaCl_2$, and 10 3-*N*-(morpholino)propanesulphonic acid (MOPS), adjusted to pH 7.5 with NaOH at 15°C. For voltage clamping, a neuron was impaled with a single-barreled voltage electrode and a double-barreled electrode. One barrel of the electrode was filled with a solution of 3 M KCl and served to pass current. The other barrel was filled with 0.2 M cAMP and 20 mM Tris buffer, adjusted to pH 7.3 with KOH, for iontophoretic injection of cAMP. All experiments were performed at a holding potential of −50 mV.

For intracellular pressure injection of cAMP, an additional electrode was filled with the cAMP solution. A pulse of positive pressure was applied manually with a syringe through polyethylene tubing. In most experiments, cAMP was iontophoretically injected with a constant current source that metered the iontophoretic current amplitude.

Known volumes of a 1 mM stock solution of the PDE inhibitor isobutylmethylxanthine (IBMX) were mixed in the bath to desired final concentrations. Since IBMX induced a persistent inward current that developed slowly, the $I_{Na,cAMP}$ responses were only measured from the plateau of the IBMX-induced inward current.

Diameters of neuron somata were estimated with an ocular micrometer. Assuming an

iontophoretic transfer number near 0.1, the final concentrations of cAMP injected into the neurons reported here might have varied from 40 to 260 μM if degradation were totally inhibited. For experiments involving movement of the tip of the intracellular iontophoretic electrode, the distance between the tip and the cell membrane was estimated with a micrometer readout on the micromanipulator, taking as zero the point where the electrode tip first contacted the cell surface. The electrode tip was positioned at the estimated cell center unless specified otherwise.

The Diffusion–Reaction Model: cAMP Concentration Change at the Membrane

In the diffusion–reaction model the time course of cAMP concentration change at the cell membrane after injection is determined by both diffusion and degradation. PDE activity is assumed to be homogeneously distributed throughout the cell volume and hydrolyzes cAMP in a first-order reaction.

Injected cAMP is assumed to diffuse spherically and isotropically within the soma. The impermeability of the cell membrane to cAMP imposes a reflective boundary condition which is mostly ignored in the present treatment. The system is simplified by assuming diffusion of cAMP in an infinite medium, because of the large size of molluscan neurons and the relatively high PDE activity. Justification for this and discussion of a more accurate equation is presented in Appendix A. In the present case, cAMP concentration at the inner membrane surface after instantaneous cAMP release from a point source is

$$C(r, t) = Q/[(4\pi Dt)^{3/2}] \exp(-r^2/4Dt) \exp(-k_{h*}t) \quad (1)$$

(cf. Carslaw and Jaeger, 1959; Purves, 1977), where Q is the amount of injected cAMP, D the effective diffusion constant for cAMP, and r the cell radius, and k_{h*} is taken as the PDE activity as estimated from the decay rate of the cAMP response. As discussed in Appendix A, k_{h*} is an underestimation that approximates the actual PDE rate constant at higher values of PDE activity and cell radius. A factor of 2 is applied to partially simulate reflection of cAMP diffusion at the cell membrane. The diffusion–reaction equation (Eq. 1) assumes an instantaneous release of cAMP from a centered point source. However, after $t > 5t'$ the solution to a diffusion equation for a continuous release with a duration of t' is not much different from one involving an instantaneous point source (Jaeger, 1965). Since the time course of the $I_{Na,cAMP}$ response is much longer than the cAMP injection duration, Eq. 1 is a very close approximation.

The Dose–Response Relation

Establishing a dose–response relation for cAMP activation of the $I_{Na,cAMP}$ response permits estimation of the stoichiometry of ligand gating. Degradation of cAMP is assumed to be rate limiting for activation of $I_{Na,cAMP}$ under normal conditions, as it is at low levels of PDE inhibition (see Results). Thus, $I_{Na,cAMP}$ amplitude is taken to reflect the cAMP concentration at the cell membrane at any moment. Accordingly, cAMP binding and dissociation and channel opening and closing are considered to be in steady state with respect to cAMP concentration. In this case, the $I_{Na,cAMP}$ amplitude may be related to the cAMP concentration by the Hill equation:

$$I_{Na,cAMP} = I_{max}C^n/(C^n + K_C^n) \quad (2)$$

where $I_{max} = Ng(E - E_{Na})$. Here, N is the total number of channels, g the single channel conductance, E the holding potential, and E_{Na} the Na^+ reversal potential. n is the stoichiometric ratio of cAMP binding to the channel, the Hill coefficient as described below. K_C is the apparent dissociation constant for cAMP binding. C is the increase in cAMP concentration at the cell membrane after injection, and is determined by Eq. 1.

In practice, the dose–response relation is obtained by recording the $I_{Na,cAMP}$ amplitude as a

function of iontophoretic current duration and amplitude. Eq. 2 may be redefined in those terms, since the amount of injected cAMP is proportional to the product of the iontophoretic current amplitude (I_a) and duration (I_d). Thus, the empirical dose–response relation expressing $I_{Na,cAMP}$ amplitude as a function of I_a or I_d is:

$$I_{Na,cAMP} = I_{max} I_i^n / (I_i^n + K_i^n) \quad (3)$$

where I_i is either a variable I_a when I_d is held constant or a variable I_d at constant I_a, and K_i is the apparent dissociation constant defined in terms of the value of I_a or I_d, determined experimentally (see Fig. 4). When the dose–response relation is plotted in double log form, its slope is the Hill coefficient describing the cooperativity for cAMP binding to the channel receptor.

Data Analysis

The dose–response relations of $I_{Na,cAMP}$ were curve-fitted with Eq. 3 using a least-squares algorithm (Schiff, 1985) expressing the apparent dissociation constants K_a and K_d in terms of I_a and I_d, respectively.

The time course of a single $I_{Na,cAMP}$ response to a very short pulse of cAMP injection was fitted by eye using the diffusion–reaction equation (Eq. 1). The injection current was kept low to satisfy the condition $C \ll K_C$; thus, Eq. 3 could be reduced to $I_{Na,cAMP} = (I_{max}/K_C)\, C^n$. The value of I_{max}/K_C was constant for these experiments (all $I_{Na,cAMP}$ responses were obtained at the holding potential of −50 mV), and Eq. 1 was used to generate the theoretical curve. The decay rate constant $k_{h'}$ was measured from the decay phase of the $I_{Na,cAMP}$ response, and r, the cell radius, was measured optically. The only free parameter was the effective cAMP diffusion coefficient D, the value of which ($3.3 \cdot 10^{-6}$ cm^2/s) was obtained after fitting the diffusion equation to the data; this value was used throughout the analyses.

The theoretical effects of an eccentrically located point source of cAMP in Fig. 6 were computed with the following equation, which is derived in Appendix B:

$$I_{Na,cAMP}(t) = 2\pi r^2 I_i \sigma \int_0^{\pi} [1 + (K_C'/Q) 4(\pi D t)^{3/2} \exp(k_{h'} t) \exp[(r^2 - 2rr' \cos\theta + r'^2)/4Dt]]^{-1} \sin\theta \, d\theta \quad (4)$$

where σ, I_i, r', and K_C' are defined as in Appendix B. Other variables are defined as previously. The equation is for the general case of diffusion from an eccentrically located source, and for simplicity no boundary conditions are included. Numerical integration of Eq. 4 was done by Romberg's method (Sauer and Szabo, 1968).

RESULTS

The Roles of Diffusion and Degradation in the $I_{Na,cAMP}$ Response to Injected cAMP

Injection of cAMP depolarized the pedal neurons and induced bursts of action potentials (Fig. 1 *A*). Recorded under voltage clamp between −100 and −20 mV, cAMP activated a slow, Na^+-dependent inward current ($I_{Na,cAMP}$) with a time course similar to depolarization in the unclamped condition (Fig. 1 *B*). $I_{Na,cAMP}$ rose to a peak within several seconds after a short pulse of cAMP and the subsequent decay phase showed a simple exponential time course.

Consistent with the kinetics of diffusion phenomena, both the time course and amplitude of the $I_{Na,cAMP}$ could be appreciably altered by moving the tip of the cAMP injection electrode between the cell membrane and the cell center. As the electrode moved from the membrane toward the center, the latencies to current onset and to

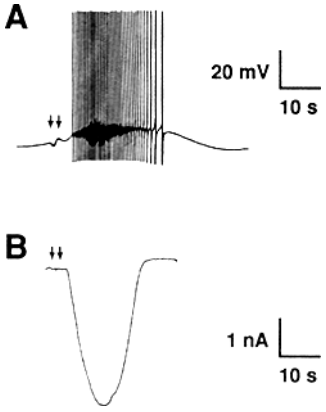

FIGURE 1. (*A*) Intracellular pressure injection of cAMP depolarized the membrane potential and induced a burst of action potentials. (*B*) A similar injection in the voltage clamped neuron elicited a transient cAMP-activated Na^+ current ($I_{Na,cAMP}$). Arrows mark the onset and end of pressure injection. Holding potential, −50 mV.

the current amplitude peak increased, while the peak current amplitude itself decreased (Fig. 2). When the cAMP injection electrode tip was approximately centered in the soma, the latency to peak $I_{Na,cAMP}$ was unaffected by varying the amount of injected cAMP (Fig. 3 *A*). However, when the electrode tip was positioned eccentrically, the latency to peak increased as the iontophoretic injection current was increased (Fig. 3 *B*). This result is interpreted below as arising from regional asymmetry in the activation of the current over the neuron membrane area. The exponential decay rates of the response remained unaltered.

The PDE inhibitor IBMX delayed attainment of peak amplitude of the $I_{Na,cAMP}$ response and slowed its decay rate (Fig. 4 *A*; $N = 6$). This is consistent with cAMP degradation being the likely rate-limiting factor in the presence of IBMX. The decay rate decreased monotonically with increasing bath concentrations of IBMX; for the results in Fig. 4, *A* and *B*, the decay rate in normal saline decreased from 0.25 s^{-1} to 0.17 s^{-1} in 10 μM IBMX. Further increases in IBMX concentration further decreased the decay rate constant of the $I_{Na,cAMP}$ responses.

At the lower concentrations, IBMX caused increases in $I_{Na,cAMP}$ peak amplitude; however, responses began to decrease at higher IBMX concentrations (Fig. 4, *A* and *B*). IBMX also induced a persistent inward current that increased with inhibitor concentration (Fig. 4, *C* and *D*). This current was reduced in low Na^+ saline. These data suggest that PDE inhibition caused accumulation of endogenously generated

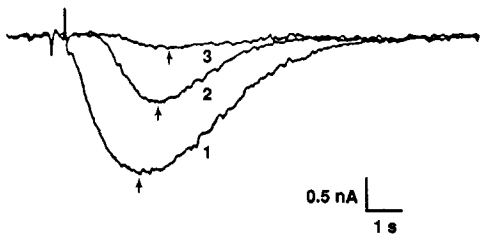

FIGURE 2. The time course and amplitude of $I_{Na,cAMP}$ changed with the distance of the injection electrode from the cell membrane. cAMP was released at estimated distances of 40 (*1*), 80 (*2*), and 120 μm (*3*) from the membrane in an approximately spherical soma of 240 μm diam. The latencies to $I_{Na,cAMP}$ response initiation and to peak amplitude (*arrows*) increased with distance, while amplitude was reduced. The rate constants of the decay phases of all responses were identical, having values of 0.7 s^{-1}. Injection amplitude, −300 nA. Injection duration, 0.6 s.

cAMP, which in turn increased the resting level of $I_{Na,cAMP}$. In this interpretation, the resulting saturation of the $I_{Na,cAMP}$ response would be due to a smaller number of channels available for recruitment.

Qualitatively similar results were obtained in three experiments using the more specific PDE inhibitor, RO20-1724 (10–50 μM).

Dose–Response Relation of $I_{Na,cAMP}$ and the Hill Coefficient

Typical dose–response relations are shown for both increasing iontophoretic current amplitude (I_a) at fixed duration (I_d) and for increasing duration at fixed amplitude (Fig. 5, *A* and *B*, *left*). Using Eq. 3, a Hill coefficient of 1.0 fitted both data sets well, consistent with 1:1 binding of cAMP to the channel receptor.

$I_{Na,cAMP}$ responses to differing pulses of cAMP injection with a fixed product of I_a and I_d had different time courses, but their amplitudes were the same (Fig. 5 *C*). The result was consistent with the expectation that the amount of injected cAMP was proportional to the product of I_a and I_d, in agreement with the derivation and use of Eq. 3.

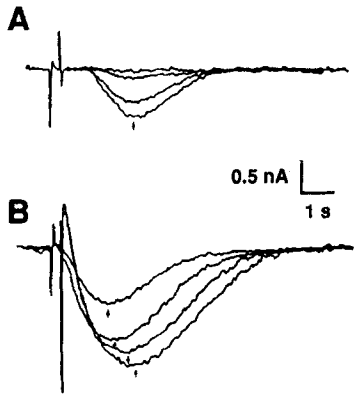

FIGURE 3. Effects of centered versus eccentric cAMP injection on the time course of $I_{Na,cAMP}$. Two sets of $I_{Na,cAMP}$ responses were elicited by 0.6-s injections of increasing amplitude: −100, −300, −600, and −900 nA. (*A*) Responses recorded from cAMP injected at the approximate center of the spherical soma. The electrode tip was positioned 120 μm from the cell membrane. (*B*) Responses recorded from an eccentrically located injection site, at a distance of 40 μm from the cell membrane.

A Diffusion–Reaction Model of $I_{Na,cAMP}$

The experimental results suggest major roles for diffusion and degradation processes in the $I_{Na,cAMP}$ response. Incorporating terms for these processes, the diffusion–reaction equation (Eq. 1) produced satisfactory fits of $I_{Na,cAMP}$ responses using the estimated Hill coefficient of 1.0 and a value of k_h, taken from the decay phase of the response (Fig. 6 *A*).

The main features of the experimental results are simulated by the diffusion–reaction equation. It describes the exponential decay of the $I_{Na,cAMP}$ response, for the decay term $\exp(-k_h t)$ comes to dominate the right-hand side of the equation as the value of t becomes large. Further, simulating movement of the iontophoretic electrode away from the cell membrane by increasing the value of r both delays the arrival and decreases the concentration of cAMP at the membrane, while leaving the decay rate unchanged. This is consistent with the experimental results of Fig. 2.

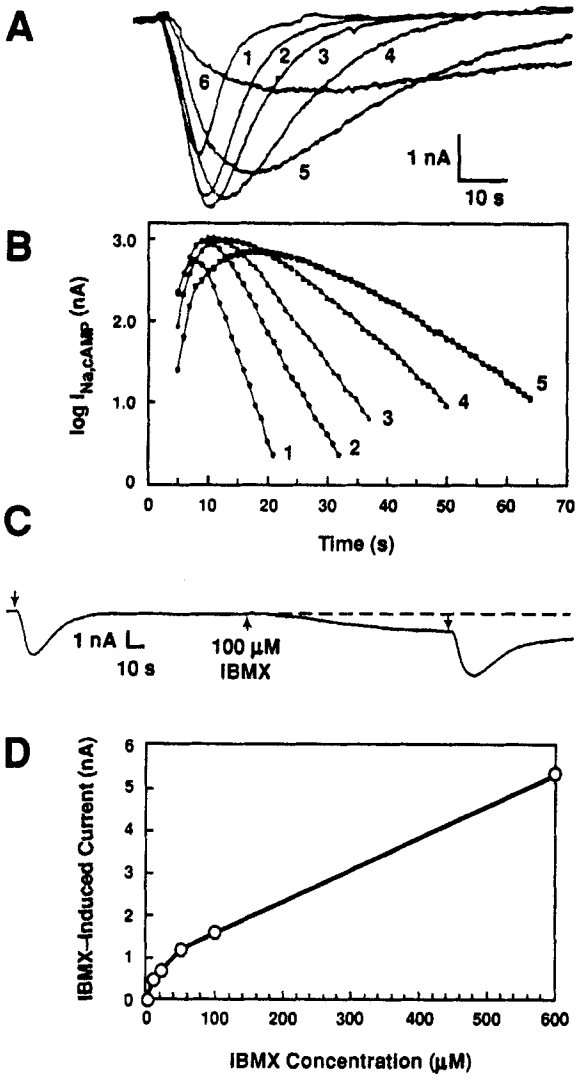

FIGURE 4. Effects of PDE inhibition on the time course of $I_{Na,cAMP}$. (*A*) Increasing concentrations of IBMX increased latencies to peak amplitude of $I_{Na,cAMP}$ responses and decreased decay rate. Peak amplitudes initially increased, and then declined. Numbers indicate $I_{Na,cAMP}$ response recordings in 0 (*1*), 10 (*2*), 20 (*3*), 50 (*4*), 100 (*5*), and 600 μM IBMX (*6*). $I_{Na,cAMP}$ responses were elicited by 5-s, 20-nA iontophoretic injections of cAMP. (*B*) Semilogarithmic plots of $I_{Na,cAMP}$ responses *1–5* (points were hand-measured). (*C*) 100 μM IBMX induced a persistent inward current believed to be of $I_{Na,cAMP}$ origin. (*D*) Dose dependence of IBMX activated persistent inward current.

Eq. 1 also predicts the increasing latency to peak amplitude (t_{max}) caused by IBMX (Fig. 4 *A*). This is shown by expressing t_{max} explicitly as a function of k_{h^*}, then taking the derivative of Eq. 1 with respect to t, equating it to zero, and then solving for t. The resulting formula reads

$$t_{max} = [(9D^2 + 4k_{h^*}Dr^2)^{1/2} - 3D]/(4k_{h^*}D) \tag{5}$$

which reduces to $r^2/6D$ as $k_{h^*} \rightarrow 0$. Thus, t_{max} increases with decreasing PDE activity (k_{h^*}), in accord with the experimental results of Fig. 4.

Likewise, the $I_{Na,cAMP}$ response peak (corresponding to peak cAMP concentration at the cell membrane, C_{max}) can be solved after substituting t_{max} for t of Eq. 1. It is

$$C_{max} = Q/4(\pi D)^{3/2}\cdot[-\alpha/(4Dk_{h^*})]^{-2/3}\cdot\exp[(3\alpha + 4r^2k_{h^*})/2\alpha] \tag{6a}$$

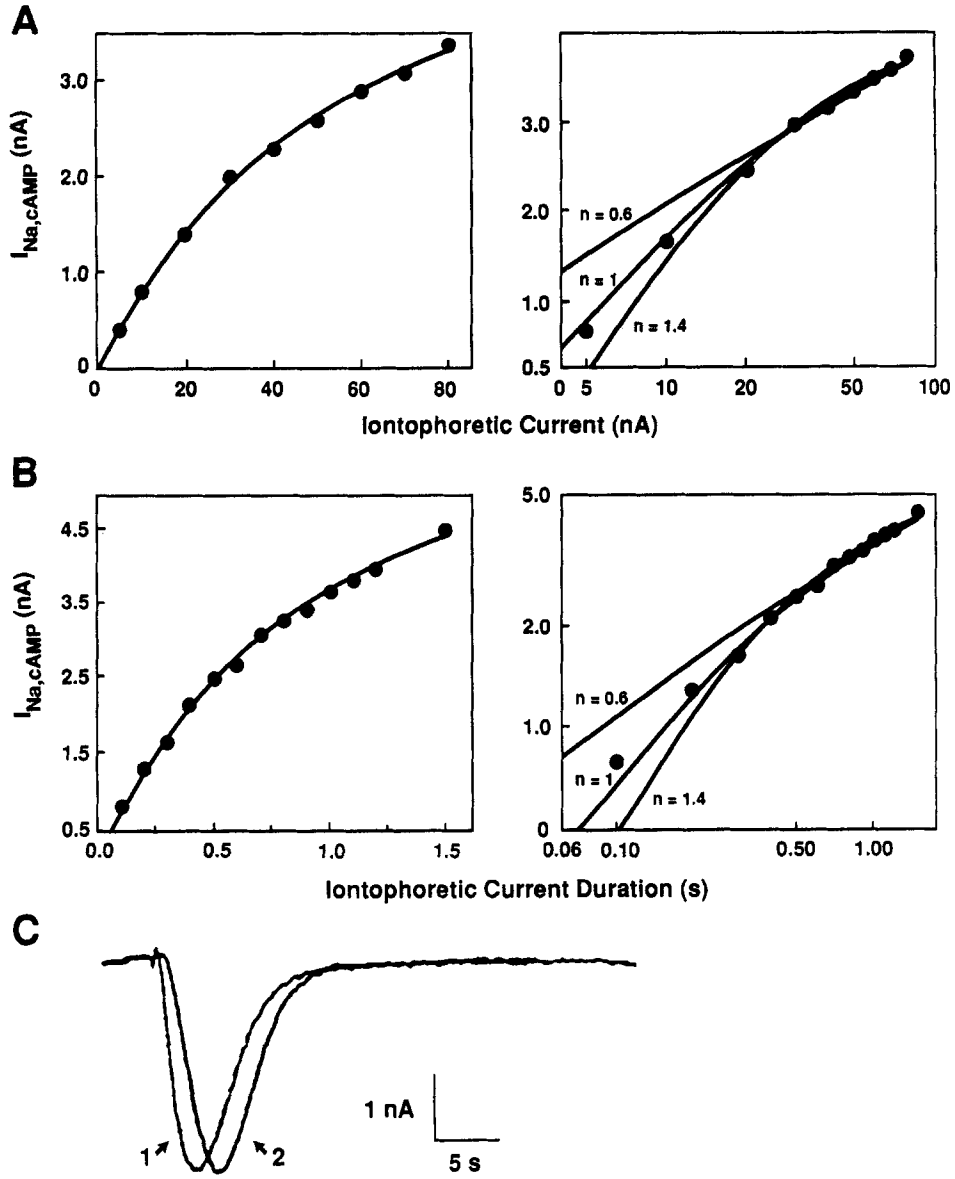

FIGURE 5. Dose–response relations of $I_{Na,cAMP}$. (*A*) *Left*, $I_{Na,cAMP}$ amplitude increased with increasing cAMP iontophoretic injection amplitude (injection duration, 2 s). The continuous curve was computed with Eq. 4, with fitted $I_{max} = -6.1$ nA and $K_a = -65.6$ nA (expressed in terms of iontophoretic injection amplitude). *Right*, The log-log plot was closely fitted with a Hill coefficient (n) of 1.0. Curves computed with coefficients of 0.6 and 1.4 are shown for comparison. (*B*) $I_{Na,cAMP}$ amplitude also increased with increasing injection duration (injection amplitude, −400 nA) (*left*). The dose–response relation was best fitted with $I_{max} = -7.3$ nA and $K_d = 0.97$ s (expressed in terms of injection duration). The corresponding log-log plot (*right*) was also fitted best with $n = 1.0$. Curves computed with coefficients of 0.6 and 1.4 are shown for comparison. (*C*) Superimposed $I_{Na,cAMP}$ responses elicited at different injection strengths and durations, with a constant strength–duration product. Response 1 was elicited by a cAMP injection of −200 nA for 0.2 s, while response 2 was elicited by a cAMP injection of −20 nA for 2 s. Although the responses differed in their latencies to peak amplitude and rates of rise, the peak amplitudes and the decay rates of the responses were the same.

where α is given by

$$\alpha = (9D^2 + 4k_{h*}Dr^2)^{1/2} - 3D \tag{6b}$$

The biphasic effects of increasing IBMX on $I_{Na,cAMP}$ amplitude can be explained and related to the model by recognizing the effect of partial saturation of the current. Eq. 6 predicts a monotonic increase in C_{max} with decreasing PDE activity (k_{h*}). Such increases were found at lower IBMX concentrations (10 and 20 μM in Fig. 4 *A*). The subsequent decreases in peak amplitude with higher IBMX concentrations, presumably due to current saturation by an increase in endogenous cAMP, are not predicted by the diffusion–reaction equation. This is simply because the equation does not take endogenous cAMP into account in its present form.

The diffusion–reaction equation may be straightforwardly modified to account for

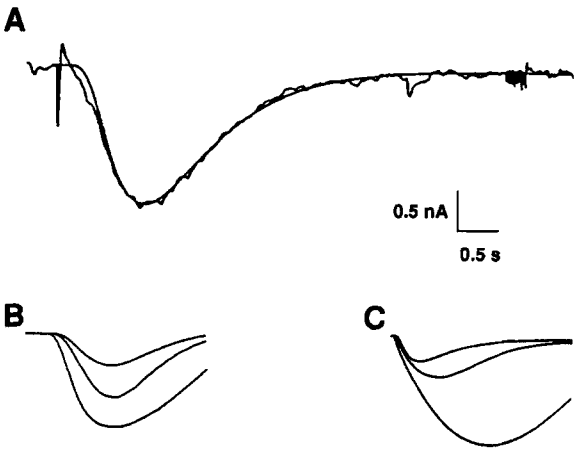

FIGURE 6. Simulations of $I_{Na,cAMP}$. (*A*) The $I_{Na,cAMP}$ response was curve-fitted with Eq. 1 and the computed curve is superimposed on the actual record. A binding stoichiometry of 1:1 was assumed. The soma radius, r, was 90 μm; the value of k_{h*} was taken as 0.56 s^{-1}, which was the slope of the exponential decay of the response. Iontophoretic injection amplitude, −640 nA; duration, 20 ms. Curves simulating the data of Fig. 5, *A* and *B* were computed with Eq. 4, with $K'_C = 6.6\ 10^{-14}$ mol and $Q = 10^{-16}$, 10^{-14}, and 10^{-12} mol in increasing order. (*B*) Curves were computed for a centrally located electrode tip ($r' = 0$), with the result that the latency to peak was independent of the value of Q. (*C*) Curves were computed for an eccentrically located electrode tip ($r' \neq 0$), with the result that the latency to peak increased with increasing value of Q.

the effects of locating the point source of injected cAMP off-center within the cell. The eccentric source will result in an eccentric gradient of cAMP in the cell, and thereby assymmetric activation of $I_{Na,cAMP}$ over the membrane area. Thus, larger injections of cAMP will activate increasingly distant channels with time, leading to larger peak response amplitudes that occur with longer latencies. This would not happen for a centered cAMP source, for which all channels of the spherical neuron will be simultaneously affected to the same extent. When the diffusion equation is modified to take into account electrode tip location and regional asymmetry in activation of the current as in Eq. 4, it qualitatively reproduces the form of the experimental results (Fig. 6, *B* and *C;* compare with Fig. 3, *A* and *B*).

DISCUSSION

The experimental data suggest that diffusion and the rate of hydrolysis are major determinants of the kinetics of $I_{Na,cAMP}$. The sensitivities to intracellular injection location of the $I_{Na,cAMP}$ response latency and latency to peak amplitude are expected properties of a diffusion phenomenon. The simple exponential decay of $I_{Na,cAMP}$ and its sensitivity to low concentrations of PDE inhibitor suggest that the decay reflects the first-order degradation of cAMP.

Saturation of $I_{Na,cAMP}$ limits the response amplitude at higher levels of injected cAMP; such a saturation effect also appears to operate at lower levels of injected cAMP when PDE is inhibited, and endogenous cAMP levels are presumed to be high. A major contribution to the decline in peak amplitude by Na^+ loading seems unlikely. Connor and Hockberger (1984) showed that the increase in $[Na^+]_i$ caused by a very large cAMP injection was only a few millimolar, which would not produce a large change in the electromotive force on the sodium ion.

The above observations served to define the system in relatively simple terms that could be described in a diffusion–reaction equation incorporating PDE activity. Experimental values were supplied as the activation stoichiometry (1 cAMP:1 $I_{Na,cAMP}$ channel), estimated from the Hill coefficient of the dose–response relation, and the first-order rate constant for PDE measured from the exponential decay of the $I_{Na,cAMP}$ response. These values were used in the model equation to successfully curve-fit the $I_{Na,cAMP}$ response. Slight modification of the model allowed for regional differences in current activation for the case of eccentric location of the point source of cAMP.

The analyses presented here have relevance to several aspects of neuronal function involving $I_{Na,cAMP}$ or similar ion currents. For instance, the likely role of the PDE enzyme in shaping $I_{Na,cAMP}$ emphasizes the interesting possibilities and consequences of the regulation of the enzyme by other intracellular messengers, posttranslational processing, or drugs. More specifically, these results and their interpretation relate to those synaptic potentials mediated through neuromodulator regulation of $I_{Na,cAMP}$. Such potentials may be much slower than postsynaptic potentials mediated by direct receptor regulation of ion channels, such as for cholinergic receptors of vertebrate skeletal muscle. It is pertinent that the model equation used here is similar to one describing the development of membrane potential in response to instantaneous deposit of charge through ion channels (Purves, 1977; Jack et al., 1983). The PDE activity represented by k_{h^*} in Eq. 1 is functionally analogous to the reciprocal of the cell membrane time constant in characterizing the electrotonic decay of membrane potential. In our study, estimated neuronal PDE activity ranged from 0.2 to 0.8 s^{-1}; thus, decay of a neuromodulator-induced potential might occur with a time constant of 1.3–5 s. The presynaptic firing rate at which significant temporal summation of $I_{Na,cAMP}$ synaptic currents will occur would depend on the postsynaptic PDE activity, and could be very low indeed.

The $I_{Na,cAMP}$ of the molluscan neuron resembles cation currents activated by cyclic nucleotides in vertebrate cells, including the cAMP-stimulated current of olfactory epithelium (Nakamura and Gold, 1987) and the cGMP-activated current of vertebrate rods (Fesenko et al., 1985; Haynes et al., 1986). It is of interest, and perhaps a reflection of evolutionary distance, that $I_{Na,cAMP}$ shows no evidence of cooperativity of

cyclic nucleotide activation, unlike the vertebrate currents where the stoichiometry of activation may be two to three cyclic nucleotide molecules binding per channel. The present work has provided some evidence of the roles of diffusion and degradation as important determinants of the kinetics of the current. The model developed from the empirical results accounts qualitatively and quantitatively for the important aspects of the current kinetics; potentially, it provides both practical and theoretical foundations for future analyses of the regulation of this class of current by neuromodulator–receptor interactions, the actions of drugs, and actions of other intracellular messenger pathways.

APPENDIX A

Eq. 1, as used here, is a convenient approximation of cAMP diffusion from a point source within a cell. However, it best describes the concentration of cAMP at a reflective surface within an otherwise infinite medium (Carslaw and Jaeger, 1959; cf. Purves, 1977) and ignores the spherical diffusion boundary of the cell membrane. It may be seen in the equation that as PDE activity goes to zero, the steady-state concentration of cAMP at $t = \infty$ would decline to zero, not $3Q/4\pi r^3$ as should be expected for a spherical cell. Where a spherical boundary exists, reflection of cAMP diffusion at the membrane requires a more complex expression for accurate description of cAMP concentration over space and time. However, as either cell size or PDE activity are increased to values like those used in this study, Eq. 1 becomes a close and convenient approximation.

A more accurate equation is available, whose predictions can be compared with those of the above equation. It is

$$C(r, t) = \left\{3Q/4\pi r^3 + Q/2\pi r^2 r' \sum_{n=1}^{\infty} [(r^2\alpha_n^2 + 1)/r^2\alpha_n^2] \sin(\alpha_n r) \sin(\alpha_n r') \exp(-D\alpha_n^2 t)\right\} \exp(-k_h t) \quad \text{(A1)}$$

(Eq. 10 of Carslaw and Jaeger, 1959) where the α_n's are the positive roots of

$$r\alpha \cdot \cot(r\alpha) - 1 = 0 \quad \text{(A2)}$$

Q is the amount of injected cAMP, D is the effective diffusion constant for cAMP, and k_h is the actual native PDE activity. The term $\exp(-k_h t)$ represents first-order degradation of cAMP by PDE activity distributed homogeneously. The first six roots of $r\alpha_n$ for Eq. A2 are

$$r\alpha_n = 0 \qquad r\alpha_n = 10.9041$$
$$r\alpha_n = 4.4934 \qquad r\alpha_n = 14.0662$$
$$r\alpha_n = 7.7253 \qquad r\alpha_n = 17.2208$$

(Carslaw and Jaeger, 1959).

Both Eqs. 1 and A1 can be used to fit the same experimental data equally well, but the fitted value of k_{h*} will always be somewhat lower than that of k_h. Nevertheless, the difference between the two values becomes smaller as the PDE activity increases and as the cell radius increases. This is shown explicitly in Table I.

Thus, at higher PDE activity and for larger cells, Eq. 1 is a useful approximation to Eq. A1. Eq. 1 permits a simplified analysis of $I_{Na,cAMP}$ kinetics, and for this reason it has been used in this study.

APPENDIX B

The derivation of Eq. 4 is similar to that used by Dreyer et al. (1978). When the iontophoretic electrode tip is taken as a point source (x', y', z') in the rectangular coordinate system, the concentration of cAMP at any point (x, y, z), after an instantaneous release of cAMP from the electrode tip, is given by

$$C(x, y, z, t) = Q/[4(\pi Dt)^{3/2}] \exp(-k_{h^*}t) \exp[-(x - x')^2 - (y - y')^2 - (z - z')^2/(4Dt)] \quad \text{(B1)}$$

where k_{h^*}, D, and Q are as defined earlier. The transformation rules for converting (x, y, z) into spherical coordinates (r, θ, ϕ) are:

$$x = r \sin\theta \cos\phi \quad \text{(B2a)}$$

$$y = r \sin\theta \sin\phi \quad \text{(B2b)}$$

$$z = r \cos\theta \quad \text{(B2c)}$$

TABLE I

Decay rate constant k_{h^*}, s^{-1}	Decay rate constant/phosphodiesterase activity (k_{h^*}/k_h)		
	Cell diameter		
	100 μm	150 μm	200 μm
0.100	0.571	0.750	0.847
0.200	0.719	0.860	0.922
0.300	0.789	0.901	0.946
0.400	0.846	0.926	0.959
0.500	0.870	0.938	0.971
0.600	0.900	0.945	0.976
0.700	0.910	0.955	0.979
0.800	0.920	0.965	0.980
0.900	0.925	0.967	0.987
1.000	0.930	0.970	0.990

The values of the decay rate of the $I_{Na,cAMP}$ response, k_{h^*}, and of the PDE activity converge with increasing cell radius and PDE activity. Calculations are presented for cells of three different radii: 100, 150, and 200 μm.

When the point source is chosen to coincide with the z axis in the spherical coordinate system, (x', y', z') becomes $(r', 0, 0)$ and Eq. B1 now reads

$$C(r, \theta, \phi, t) = Q/[4(\pi Dt)^{3/2}] \exp(-k_{h^*}t) \exp[-(r^2 - 2rr' \cos\theta + r'^2)/4Dt] \quad \text{(B3)}$$

To consider spatially distributed channels, the currents passing through all the individual channels are summated. This is done by integrating some function of Eq. B3 with respect to an area element, A. It is

$$I_{Na,cAMP}(t) = I_i\sigma \int\int_A f[C(r, \theta, \phi, t)]\, dA \quad \text{(B4)}$$

where σ is the channel density and I_i is the average current passing through an individual channel.

When current saturation is taken into account, the term $f[C(r, \theta, \phi, t)]$ in Eq. B4 is replaced by $C(r, \theta, \phi, t)/[C(r, \theta, \phi, t) + K_C']$, where K_C' is the apparent dissociation constant. Thus, Eq. B4 becomes

$$I_{Na,cAMP}(t) = I_i\sigma \int\int_A C(r, \theta, \phi, t)/[C(r, \theta, \phi, t) + K_C']\, dA$$

$$= I_i\sigma \cdot \int_0^{\pi}\int_0^{2\pi} C(r, \theta, \phi, t)/[C(r, \theta, \phi, t) + K_C']r^2 \sin\theta\, d\phi\, d\theta$$

$$= 2\pi r^2 \cdot I_i\sigma \cdot \int_0^{\pi} 1/[K_C'/C(r, \theta, \phi, t) + 1] \sin\theta\, d\theta \quad \text{(B5)}$$

Replacing $C(r, \theta, \phi, t)$ with Eq. B3, Eq. B5 becomes

$$I_{Na,cAMP}(t) = 2\pi r^2 \cdot I_i\sigma \cdot \int_0^{\pi} [1 + (K_C'/Q)4(\pi Dt)^{3/2} \exp(k_h \cdot t)$$

$$\exp[(r^2 - 2rr' \cos\theta + r'^2)/4Dt]]^{-1} \sin\theta\, d\theta \quad \text{(B6)}$$

This is the general solution relating the $I_{Na,cAMP}$ amplitude to cAMP concentration at the cell membrane, and it may be solved by numerical integration.

The authors are grateful to Chin-Wen Hsin, Phil Best, and Martha Gillette for discussion and generous loans of equipment.

This research was supported by National Science Foundation grant BNS 86 03816.

Original version received 18 September 1989 and accepted version received 18 March 1991.

REFERENCES

Aldenhoff, J. B., G. Hofmeier, H. D. Lux, and D. Swandulla. 1983. Stimulation of a sodium influx by cAMP in Helix neurons. *Brain Research.* 276:289–296.

Carslaw, H. S., and J. C. Jaeger. 1959. Conduction of Heat in Solids. 2nd ed. Clarendon Press, Oxford, UK. 237–240, 353, 367.

Connor, J. A., and P. Hockberger. 1984. A novel membrane sodium current induced by injection of cyclic nucleotides into gastropod neurons. *Journal of Physiology.* 354:139–162.

Crank, J. 1975. The Mathematics of Diffusion. 2nd ed. Oxford University Press, 97.

Deterre, P., D. Paupardin-Tritsch, J. Bockaert, and H. M. Gerschenfeld. 1981. Role of cyclic AMP in a serotonin-evoked slow inward current in snail neurones. *Nature.* 290:783–785.

Dreyer, F., K. Peper, and R. Sterz. 1978. Determination of dose-response curves by quantitative iontophoresis at the frog neuromuscular junction. *Journal of Physiology.* 281:395–419.

Fesenko, E. E., S. S. Kolesnikov, and A. L. Lyubarsky. 1985. Induction by cyclic GMP of cationic conductance in plasma membrane of retinal rod outer segment. *Nature.* 313:310–313.

Gillette, R., and D. J. Green. 1987. Calcium dependence of voltage sensitivity in adenosine 3′,5′-cyclic phosphate-stimulated sodium current. *Journal of Physiology.* 393:233–245.

Gillette, R., and R.-C. Huang. 1988. Co-regulation of $I_{Na,cAMP}$ by cAMP and Ca^{2+}: a competitive binding mechanism. *Society for Neuroscience Abstracts.* 14:438.18. (Abstr.)

Green, D. J., and R. Gillette. 1983. Patch and voltage clamp analysis of cAMP-stimulated inward current underlying neurone bursting. *Nature.* 306:784–785.

Green, D. J., and R. Gillette. 1988. Regulation of cyclic AMP-dependent ion current by intracellular pH, calcium and calmodulin blockers. *Journal of Neurophysiology.* 59:248–258.

Hara, N., M. Sawada, and T. Maeno. 1985. Influences of pressure-injected cyclic AMP on the membrane current and characteristics on the identified neurons of *Aplysia kurodai*. *Japanese Journal of Physiology*. 35:985–1012.

Haynes, L. W., A. R. Kay, and K.-W. Yau. 1986. Single cyclic GMP-activated channel activity in excised patches of rod outer segment membrane. *Nature*. 321:66–70.

Huang, R.-C., and R. Gillette. 1989. cAMP activates slow Na^+ current without phosphorylation. *Society for Neuroscience Abstracts*. 19:514.2. (Abstr.)

Jack, J. J. B., D. Noble, and R. W. Tsien. 1983. Electric Current Flow in Excitable Cells. Clarendon Press, Oxford.

Jaeger, J. C. 1965. Diffusion from constrictions. *In* Studies in Physiology. D. R. Curtis and A. K. McIntyre, editors. Springer-Verlag, Berlin. 106–117.

Kononenko, N. I., P. G. Kostyuk, and A. D. Scherbatko. 1983. The effect of intracellular cAMP injections on stationary membrane conductance and voltage- and time-dependent ionic current in identified snail neurons. *Brain Research*. 376:239–245.

Liberman, E. A., S. V. Minina, and K. V. Golubtsov. 1975. The study of metabolic synapse. I. Effect of intracellular microinjection of 3′,5′ AMP. *Biophysics (Moscow)*. 20:451–457.

McCrohan, C. R., and R. Gillette. 1988*a*. Cyclic AMP-stimulated sodium current in identified feeding neurons of *Lymnaea stagnalis*. *Brain Research*. 438:115–123.

McCrohan, C. R., and R. Gillette. 1988*b*. Enhancement of cyclic AMP-stimulated sodium current by the convulsant drug pentylenetetrazol. *Brain Research*. 452:21–27.

Nakamura, T., and G. H. Gold. 1987. A cyclic nucleotide-gated conductance in olfactory receptor cilia. *Nature*. 325:442–444.

Purves, R. D. 1977. The time course of cellular responses to iontophoretically applied drugs. *Journal of Theoretical Biology*. 65:327–344.

Sauer, R., and I. Szabo. 1968. Mathematische Hilfsmittel des Ingenieurs. Part III. Springer Verlag, Berlin. 301–304.

Schiff, J. D. 1985. A simple program in BASIC for least-square fitting of certain equations to experimental data. *International Journal of Bio-Medical Computing*. 16:143–148.